Molecular Crystals
Publication details, including instructions for authors and subscription information:
http://www.tandfonline.com/loi/gmcl15

Paramagnetic Relaxation of Trapped Electrons in Gamma-Irradiated Organic Glasses

D. H. Chen [a b] & Larry Kevan [a]

[a] Department of Chemistry, University of Kansas, Lawrence, Kansas, 66044

[b] Department of Chemistry, University of Southampton, England

Version of record first published: 21 Mar 2007.

To cite this article: D. H. Chen & Larry Kevan (1969): Paramagnetic Relaxation of Trapped Electrons in Gamma-Irradiated Organic Glasses, Molecular Crystals, 9:1, 183-196

To link to this article: http://dx.doi.org/10.1080/15421406908082738

Paramagnetic Relaxation of Trapped Electrons in Gamma-Irradiated Organic Glasses

D. H. CHEN‡ AND LARRY KEVAN

Department of Chemistry,
University of Kansas,
Lawrence, Kansas 66044

Abstract—Paramagnetic relaxation characteristics of trapped electrons in γ-irradiated, glassy methanol, ethanol and 2-methyltetrahydrofuran (MTHF) at 73 °K were studied by power saturation techniques. The spin-spin relaxation time is constant with radiation dose at low doses and decreases at higher doses. Together with data on the total spin concentration the results are interpreted in terms of a " spur " model in which the initial spatial distribution of radiation-produced, trapped electrons and radicals is non-uniform. According to this model the spur radius is about 59 Å in methanol and 72 Å in MTHF. These radii compare with 42 Å for trapped electrons in alkaline ice. The radius within which electrons are trapped appears to increase with decreasing polarity of the matrix. The ratio of local spin concentration to the sample average spin concentration is greater than one at low doses in all matrices.

1. Introduction

Gamma-rays deposit radiation energy inhomogeneously in condensed systems and produce an initial inhomogeneous distribution of energetic, ionized and excited species. For very fast chemical reactions the initial spatial inhomogeneity of the species involved must be taken into account. In many irradiated, frozen or solid systems, radical and ionic species are trapped and can be detected by EPR and/or optical spectroscopy. If the species are trapped quite close to their point of formation, the trapped species can exhibit spatial inhomogeneity, the extent of which relates to the trapping efficiency in the system under investigation.

‡ Present address: Department of Chemistry, University of Southampton, England.

Recently we showed how paramagnetic relaxation experiments can give useful and semi-quantitative insights into the spatial distributions of trapped electrons and hydrogen atoms in frozen aqueous systems.[1–5] Trapped electrons in irradiated alkaline ices at 77 °K show no change in their relaxation time over a range of γ-dose from 0.2 to 4 Mrad even though the electron concentration increases linearly in this range; this implies that the average spin-spin interaction and the local concentration of electrons remains constant in this dose range. The results are explained by an inhomogeneous distribution of electrons trapped in radiation-produced regions of high local radical concentration called spurs in which only intraspur spin-spin interactions are important.[1,2] At higher doses the spurs overlap, interspur spin-spin interactions become important and the relaxation time decreases with dose. In contrast, trapped hydrogen atoms in irradiated acidic ices at 77 °K exhibit a decreasing relaxation time and a linearly increasing concentration over a radiation dose range of 0.3 to 5 Mrad.[3,4] This is the behavior expected for a homogeneous distribution of trapped species. The trapped hydrogen atoms are trapped only near acidic oxyanions and undissociated acid molecules and are expected to have a uniform spatial distribution. The relaxation results confirm this.

Radiation-produced electrons are also produced in organic glasses at 77 °K such as alcohols[6] and 2-methyltetrahydrofuran[7–9] (MTHF) and can be detected by optical and EPR spectroscopy. We report here the paramagnetic relaxation characteristics of trapped electrons in these organic glasses. The radiation dose dependence of the relaxation time gives information about spatial distributions, while the relaxation time magnitudes and the linewidths give information about the nature of the electron trapping site. A revealing correlation has been found between the size of the spatial inhomogeneities associated with radiation-produced trapped electrons and the polarity of the matrix.

2. Theory

Portis[10] has classified the types of paramagnetic line broadening as homogeneous or inhomogeneous. An EPR line is homogeneously broadened by interactions which allow the spin system to remain in

thermal equilibrium during resonance absorption. Inhomogeneous line broadening interactions with nuclear spins cause different sets of electron spins to see different net local magnetic fields. Each such set of electron spins forms a " spin packet " and the observed spectrum of the total spin system is an envelope of the superimposed spin packets. The shape of the envelope depends on the intensity distribution of local magnetic fields seen by the electron spins and the ratio of spin packet width to the envelope width. If the spin packet width is much less than the envelope width, as is often observed, and if the spin packets do not interact magnetically, then the envelope shape is dependent only on the intensity distribution of local magnetic fields and is Gaussian.

An electron spin system saturates when the population ratio between the upper and lower spin energy states deviates from its thermal equilibrium value. Power saturation is most readily studied by obtaining saturation curves which are plots of EPR signal intensity versus microwave magnetic field, H_1. A study of saturation behavior allows one to determine the product T_1T_2 or sometimes T_2 alone; T_1 is the spin-lattice relaxation time and T_2 is the spin-spin relaxation time. The relevant theory for obtaining relaxation times from saturation curves under slow passage conditions has been summarized in a previous paper.[2]

Theoretical saturation curves are shown in Fig. 1. For the case of homogeneous broadening T_1T_2 can be calculated from Eq. (1)

$$T_1T_2 = 1/\gamma^2H_{\frac{1}{2}}^2 \tag{1}$$

where γ is the gyromagnetic ratio of the electron and equals 1.76×10^7 gauss^{-1} sec^{-1}, and $H_{\frac{1}{2}}$ is the value of H_1 at which the EPR signal intensity is one-half of what it would have been in the absence of saturation. Ideal inhomogeneous broadening behavior occurs when the spin packet width is much smaller than the overall linewidth. For this case T_1T_2 is calculated by Eq. (2).

$$T_1T_2 = 3/\gamma^2H_{\frac{1}{2}}^2 \tag{2}$$

The intermediate case shown in Fig. 1 corresponds to nonideal inhomogeneous broadening; Castner's analysis[11] may be applied to this case by using curve fitting procedures to correct $H_{\frac{1}{2}}$ and then

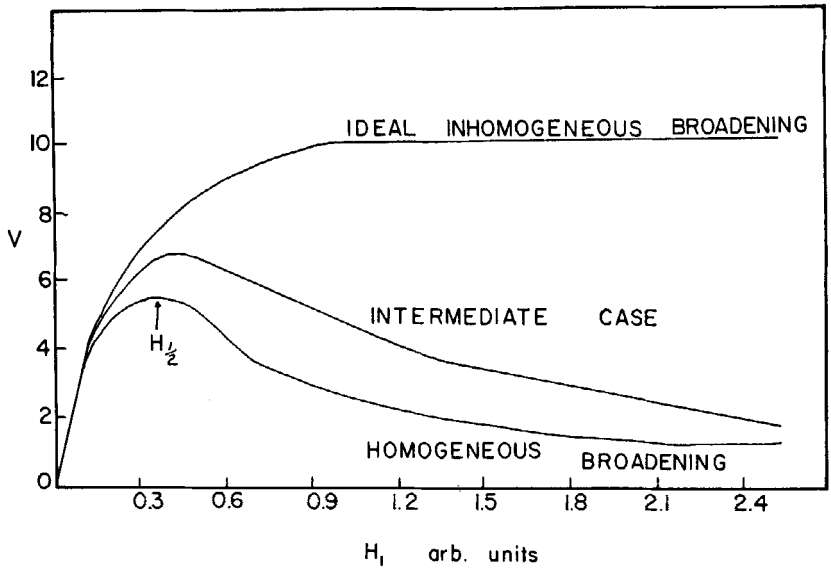

Figure 1. Power saturation curves for EPR signal intensity, V, versus microwave magnetic field, H_1: upper-theoretical curve for ideal inhomogeneously broadened EPR lines; middle-theoretical curve for nonideal inhomogeneously broadened EPR lines; lower-theoretical curve for homogeneously broadened EPR lines.

using Eq. (1) to obtain T_1T_2. This method also allows the separate calculation of T_2 from Eq. (3)

$$T_2 = \frac{1.70}{a\gamma \Delta H^G_{ms}} \tag{3}$$

where ΔH^G_{ms} is the measured linewidth at maximum slope of the observed Gaussian line and a is a measure of the ratio of the Lorentzian spin packet width to the observed Gaussian linewidth; a is determined from the saturation curve.[11]

3. Experimental

Reagent grade methanol, ethanol and MTHF were degassed on a vacuum line and dried over a freshly formed sodium film. Most methanol and ethanol samples were prepared as $\sim$2 mm glassy spheres by dropping drops of the solution into liquid nitrogen; this involved a short exposure to air. MTHF samples were

prepared by sealing into 3 mm o.d. Spectrosil quartz ampoules or by making glassy spheres without exposure to air. The latter was accomplished by pressurizing the vacuum line with dry nitrogen to force out drops through a greaseless stopcock into liquid nitrogen; the short distance between the stopcock and the liquid nitrogen surface was purged with dry nitrogen.

Irradiations were carried out at 77 °K in a U.S. Nuclear Co^{60} γ-irradiator at a dose rate of 0.51 Mrad/hr. as determined by ferrous sulfate dosimetry.

The slow passage progressive saturation measurements were made as described before[2] at 73 °K. Bubbling of liquid nitrogen was prevented by using a helium gas stream. Slow passage conditions were achieved by operating with a field modulation frequency of 40 hz and a typical modulation amplitude of 0.5 gauss. Progressive saturation curves were obtained by normalizing the EPR signal heights to a constant amplifier gain setting and plotting these heights versus microwave magnetic field, H_1. H_1 was measured as described previously.[2] Each sample using spheres utilized 3–5 spheres. Most samples were run in duplicate or triplicate.

4. Results

The EPR spectrum of γ-irradiated methanol at 77 °K consists primarily of a triplet. This triplet is shown in Fig. 2 and is due to the CH_2OH radical superimposed on a singlet due to e_t^-. Two small outer lines are also noted in the figure; these are split by 130 gauss and are due to the CHO radical. Their yield is very small. The CH_2OH radical spectrum has a theoretical 1:2:1 intensity ratio. The excess intensity in the center line is due to the trapped electron; this can be demonstrated by optical bleaching in the visible of the trapped electron line.[6] The radical spectrum was manually subtracted from the total spectrum to obtain the trapped electron signal intensity as a function of microwave power. This procedure led to relatively consistent results although the accuracy is not high. The trapped electron line in methanol had a linewidth at maximum slope of 11 gauss and a line shape that was approximately Gaussian. Figure 3 shows a typical power saturation curve for the trapped electron in methanol.

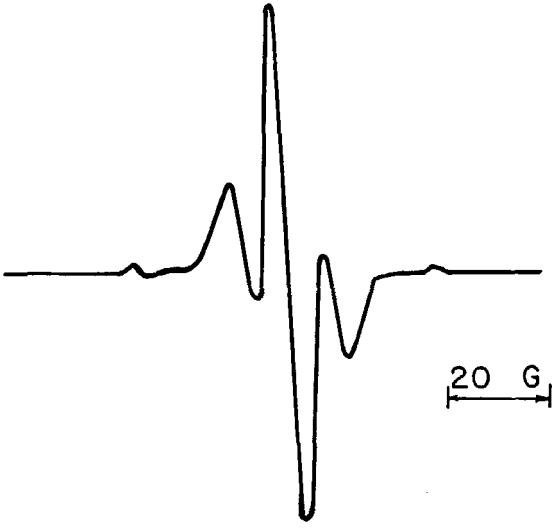

Figure 2. EPR spectrum of γ-irradiated glassy methanol at 73°K (dose 1.0 Mrad).

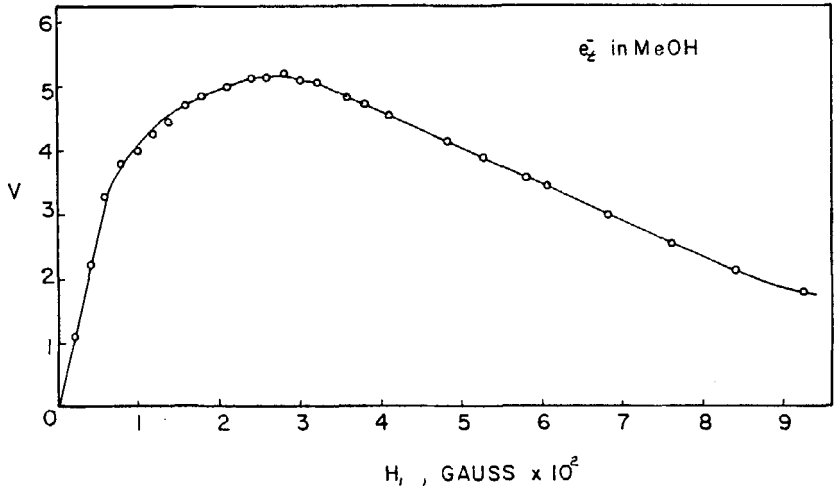

Figure 3. Slow passage power saturation curve for e_t^- in glassy methanol at 73°K (1.0 Mrad).

The relaxation times were calculated from the saturation curves by two methods. Method 1 was the Portis method in which ideal inhomogeneous broadening behavior was assumed and Eq. (2) was

used. The second method was Castner's analysis of the nonideal inhomogeneous broadening case.[11]

The EPR spectrum of γ-irradiated MTHF is shown in Fig. 4. The

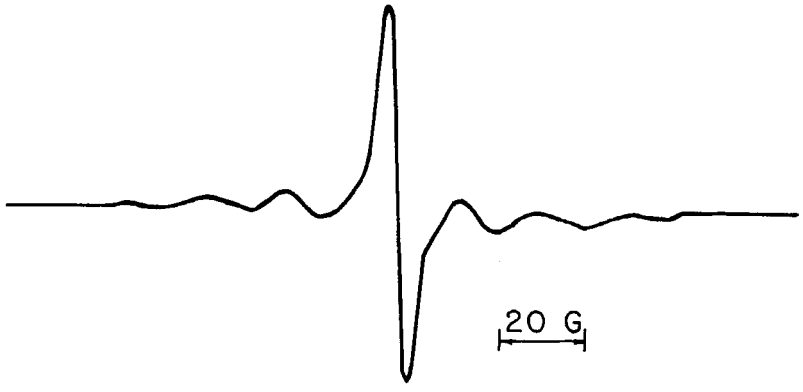

Figure 4. EPR spectrum of γ-irradiated glassy MTHF at 73 °K (dose 0.5 Mrad).

MTHF spectrum consists of a singlet e_t^- line superimposed on a 7-line radical spectrum. The 7-line radical spectrum has been interpreted as due to a free radical site at the number two carbon position. The hyperfine is then due to three methyl protons and one of the beta CH_2 protons with splitting constant A, and the other beta CH_2 proton with splitting constant $2A$, to give intensities of 1:4:7:8:7:4:1. As can be seen in Fig. 4 the e_t^- line is much more intense than the underlying radical spectrum so that the radical spectrum can be easily and accurately subtracted from the total spectrum. Thus the results obtained for e_t^- in MTHF are much more accurate than those obtained for e_t^- in methanol. The trapped electron in MTHF had a linewidth at maximum slope of 3.8 ± 0.2 gauss and had a line shape parameter[2,12] of 2.2 which indicated that it was closely Gaussian. A typical power saturation curve for e_t^- in MTHF is shown in Fig. 5.[13] Note that the peak of the saturation curve in MTHF occurs at a value of H_1 five times lower than in methanol. The MTHF saturation curves were analyzed by both Portis' and Castner's methods.

A few experiments were also done on ethanol. It exhibits a 5-line radical spectrum superimposed on a singlet trapped electron spectrum. Saturation curves were obtained by subtracting the radical spectrum

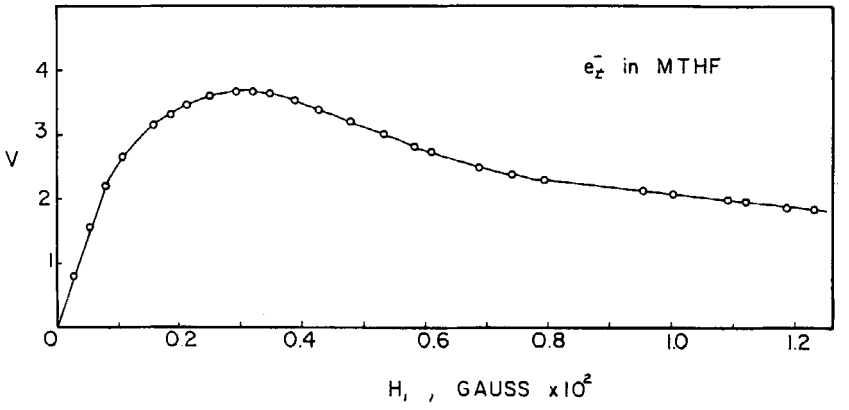

Figure 5. Slow passage power saturation curve for e_t^- in glassy MTHF at 73 °K (0.5 Mrad).

from the total spectrum but the accuracy was not high. In general, the results in ethanol paralleled those in methanol.

Table 1 summarizes the parameters determined for the trapped electrons in the various matrices. Note that the relaxation times

TABLE 1 Parameters for Trapped Electron EPR Lines in Various γ-Irradiated Matrices at 73 °K[a]

Matrix	Linewidth[b] (gauss)	Line shape	Portis' $(T_1T_2)^{\frac{1}{2}}$, sec[c]	Castner's $(T_1T_2)^{\frac{1}{2}}$, sec[d]	Castner's a	T_2, sec
10 M NaOH//H_2O[e]	13.6 ± 0.5	× Gaussian	2.2×10^{-5}	1.8×10^{-5}	0.14	5.1×10^{-8}
Methanol	11 ± 2	× Gaussian	5.2×10^{-6}	4.8×10^{-6}	~0.4	1.8×10^{-8}
Ethanol	13 ± 2	× Gaussian	4.4×10^{-6}	—	~0.4	1.5×10^{-8}
Ethanol-d_6	5 ± 1.5	× Gaussian	—	—	—	—
MTHF	3.8 ± 0.2	× Gaussian	3.6×10^{-5}	3.3×10^{-5}	0.27	0.94×10^{-8}

[a]. 0.5 Mrad dose. [b]. ΔH_{ms}^{G}. [c]. Calculated from Eq. 2.
[d]. Calculated according to Reference 11. [e]. Reference 2.

for the electrons in the alcohols are about an order of magnitude smaller than the relaxation times for trapped electrons in MTHF or in the sodium hydroxide ice. All of the results in Table 1 are at doses low enough to be in the dose independent region of the relaxation times.

Figure 6 shows the variation of relaxation time versus radiation dose. Determinations of T_2 from Eq. (3) show that the dose varia-

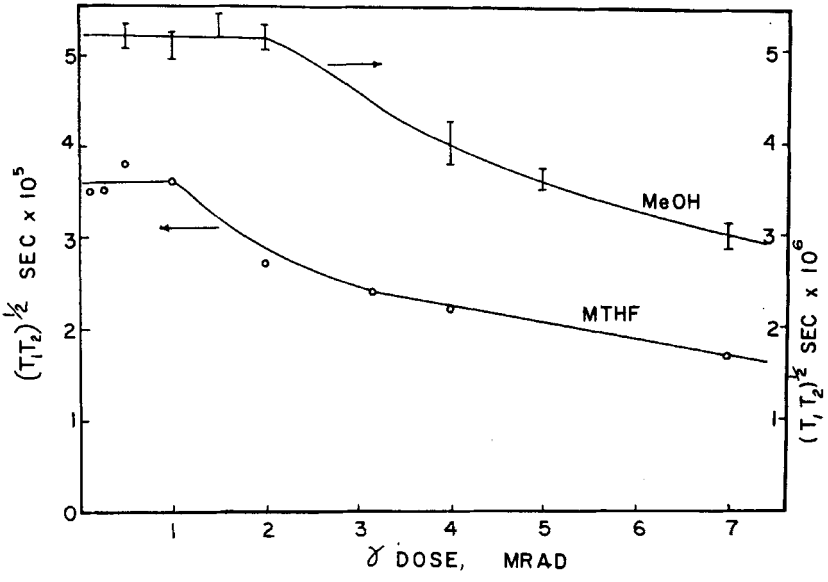

Figure 6. Relaxation time versus gamma dose of e_t^- in glassy methanol and glassy MTHF at 73°K.

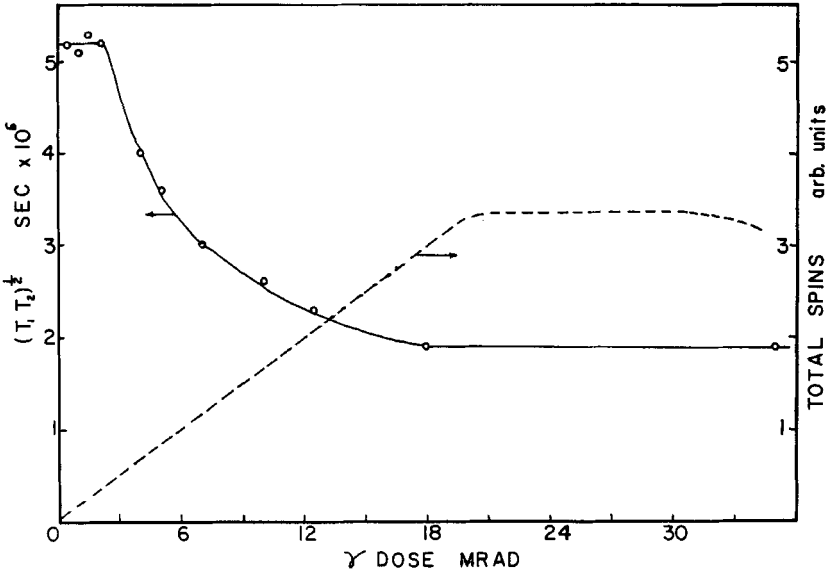

Figure 7. Relaxation time of e_t^- in glassy methanol and total spin concentration in glassy methanol versus gamma dose at 73°K.

tions in $(T_1T_2)^{\frac{1}{2}}$ are due largely to variations in T_2. In Fig. 6, however, values of $(T_1T_2)^{\frac{1}{2}}$ determined by Portis' method are plotted since they could be determined for a greater number of samples. Note that the relaxation time for electrons in methanol remains constant from 0.5 to 2.0 Mrad and then decreases. In contrast, the relaxation time for electrons in MTHF remains constant only from 0.1 to 1.0 Mrad before decreasing. Both of these contrast with the results of trapped electrons in alkaline ices[2] in which the relaxation time remains constant to about 4 Mrad dose. Figure 7 shows relaxation data for electrons in methanol extended to very high doses and also shows the total spin concentration. The decrease in the relaxation time levels off at the same dose at which the increase in the total spin concentration reaches a plateau.

5. Discussion

A. Line Shape and Broadening Mechanism

The line shape of e_t^- in MTHF fits a Gaussian function quite well according to both our data and the data of others.[9] This line shape is maintained at doses up to 6 Mrads; at higher doses it deviates slightly from a good Gaussian fit. The line shape of e_t^- in methanol and ethanol is also Gaussian. However, the fit cannot be determined precisely because of overlap with the CH_2OH radical. The e_t^- EPR linewidths in MTHF, methanol and ethanol do not increase appreciably during power saturation. At the higher microwave powers small increases in the e_t^- linewidths would be undetectable because of the increased size of the radical signal relative to that of e_t^-. However, it is clear that the e_t^- lines do not broaden with H_1 to the extent theoretically predicted for homogeneously broadened lines.

These two results imply that the e_t^- EPR lines are broadened mainly by inhomogeneous mechanisms. The shape of the power saturation curves in Figs. 3 and 5 are consistent with this conclusion. Analysis of the saturation curves by Castner's method[11] give values of his a parameter of less than one which indicate that the spin packet width is not negligible compared to the total linewidth. The most likely inhomogeneous broadening mechanisms of importance are unresolved hyperfine interaction with surrounding protons and

anisotropy broadening. The former mechanism can be evaluated semi-quantitatively from deuterated compounds.[4] The linewidth of e_t^- in ethanol-d_6 is about 5 gauss; a precise value cannot be obtained due to interference by the radical spectrum. Deuterated MTHF was not examined due to its prohibitive cost. Although quantitative analysis is not justified, the large linewidth decrease in ethanol-d_6 does indicate that unresolved hyperfine interaction is probably the dominant broadening mechanism.

B. Dose Effects on Spatial Distributions of e_t^- and Radicals

Studies in which relaxation time is measured as a function of radiation dose yield information about interactions between unpaired electron spins. For a uniform distribution of trapped species the average distance between them decreases with increasing radiation dose, and the spin-spin interaction becomes stronger. In this case T_2 is expected to decrease with increasing dose. This behavior is observed for trapped H atoms in acidic ices.[4] However, Fig. 6 shows that T_2 for e_t^- in polar organic glasses behaves somewhat differently. For e_t^- in MTHF and in methanol the dose variation in $(T_1T_2)^{\frac{1}{2}}$ is due to a variation in T_2. The important result is that $(T_1T_2)^{\frac{1}{2}}$ for e^- in methanol remains constant at 4.8×10^{-5} sec from 0.5 to 2.0 Mrad dose before decreasing. Similarly $(T_1T_2)^{\frac{1}{2}}$ for e_t^- in MTHF remains constant at 3.3×10^{-5} sec from 0.1 to 1.0 Mrad before decreasing.

The constancy of $(T_1T_2)^{\frac{1}{2}}$ over a given dose range indicates that e_t^- has spin-spin interactions with unpaired spins very close to it and only weakly interacts with other much more distant spins. This suggests that the spins are trapped in radiation-produced regions of inhomogeneity which we shall call spurs. At higher doses the spurs overlap and $(T_1T_2)^{\frac{1}{2}}$ begins to decrease. Similar results and interpretation have been reported for e_t^- in alkaline ice.[2]

The inverse relationship between the variation in $(T_1T_2)^{\frac{1}{2}}$ for e_t^- and the total spin concentration with radiation dose is demonstrated for methanol in Fig. 7. The total spin concentration includes e_t^- and CH_2OH spins; both types of spins have the same dose-yield dependence so it is undecided whether one or both spin types undergo relaxation with e_t^-. Note that as the total spin concentration

reaches a limiting maximum value above 18 Mrad, the dose variation in $(T_1T_2)^{\frac{1}{2}}$ also reaches a limiting minimum value.

A semi-quantitative measure of the spur size may be obtained from the dose at which $(T_1T_2)^{\frac{1}{2}}$ begins to decrease. This dose is 1 Mrad in MTHF, 2 Mrad in methanol and about 4 Mrad in alkaline ice.[2] We assume that at these doses the spurs just overlap to fill the entire volume and that there are $G(e_t^-)$ electron spins per spur where G is the yield per 100 eV of absorbed radiation energy. This implies that the average energy deposited per spur is 100 eV. Then the spur radius in angstroms is given by

$$r(\text{Å}) = \left(\frac{4.8 \times 10^6}{4\pi D\rho}\right)^{\frac{1}{3}}$$

where ρ is the density and D is the dose in Mrad at which $(T_1T_2)^{\frac{1}{2}}$ begins to decrease. The calculated spur radii are 72 Å in MTHF, 59 Å in methanol and 42 Å in alkaline ice. This calculation leads to an overestimate of the spur radii, but the trend with matrix polarity is unambiguously shown by the experimental data. As the matrix polarity decreases from alkaline ice to methanol to MTHF the size of the spurs increases and the amount of spatial nonuniformity exhibited by the trapped radicals becomes less. In a nonpolar matrix like 3-methylpentane glass, trapped electrons produced by γ-irradiation are expected to show little if any evidence of spatial inhomogeneity. The correlation between spur size and matrix polarity implies that radiation-produced electrons travel further before being trapped the less polar the matrix. This suggests that the trapping cross section or the trap density for radiation-produced electrons is higher in more polar matrices.

The dependence of $(T_1T_2)^{\frac{1}{2}}$ on radiation dose shows clearly but qualitatively that spatial inhomogeneity of trapped electrons and radicals exists. The absolute value of T_2 or equivalently, ΔH_{ms}^L, the dipolar spin packet linewidth, allows one to calculate a local spin concentration to compare with the sample average spin concentration. The value of T_2 and ΔH_{ms}^L depend on the a parameter which is only accurate to about 30% for $a > 0.2$. However, to the accuracy of a, ΔH_{ms}^L may be calculated from Eq. (4).[2]

$$\Delta H_{ms}^L = \frac{a\Delta H_{ms}^G}{1.47} \tag{4}$$

The relation between the dipolar linewidth and the local spin concentration was given by Kittel and Abrahams[14] for single crystals and was modified by Wyard[15] to apply to non-equivalent magnetic centers in glassy and polycrystalline matrices. Wyard obtains $\Delta H^L_{ms} = 32\,M$ where M is the total molarity of trapped spins contributing to the dipolar linewidth. The local molarity is then calculated from Eq. (5) and the sample average molarity

$$(\text{local})M = \frac{a\Delta H^G_{ms}}{32 \times 1.47} \tag{5}$$

is calculated from Eq. (6) where D is the dose in Mrad and ρ is the density.

$$(\text{sample average})M = \frac{(\text{total spins})G\,D\rho}{900} \tag{6}$$

TABLE 2 Spatial Distribution Data on Trapped Radicals in Various γ-Irradiated Matrices at 73 °K

Matrix	M(local)[a]	M(avg)[a]	$2G(e_t^-)$[b]	ρ, g/cc[c]	M(local)[a] / M(avg)	Dose indep. range of $(T_1T_2)^{\frac{1}{2}}$	Spur radius
10 M $NaOH/H_2O$	0.040	0.0061	4.2	1.3	6.6	4 Mrad	42 Å
Methanol	0.094	0.0060	6	0.9	16	2	59
MTHF	0.022	0.0058	5.2	1.0	3.8	1	72

[a]. Dose: 1 Mrad.
[b]. Taken as G (total spins); this may be an underestimate for methanol.
[c]. Estimated for solid phase.

The results for 1 Mrad total dose are summarized in Table 2. For each matrix M(local)/M(average) is greater than one which again indicates a non-uniform spatial distribution of trapped radicals.

Acknowledgment

This research was supported by the Air Force Rocket Propulsion Laboratory and the U.S. Atomic Energy Commission. This is AEC Document No. C00-1528-25.

REFERENCES

1. Zimbrick, J. and Kevan, L., *J. Am. Chem. Soc.* **88**, 3678 (1966).
2. Zimbrick, J. and Kevan, L., *J. Chem. Phys.* **47**, 2364 (1967).
3. Zimbrick, J. and Kevan, L., *Nature* **214**, 693 (1967).
4. Zimbrick, J. and Kevan, L., *J. Chem. Phys.* **47**, 5000 (1967).
5. Kevan, L. and Chen, D. H., *J. Chem. Phys.* **49**, 1970 (1968).
6. Chachaty, C. and Hayon, E., *Nature* **200**, 59 (1963).
7. Ronayne, M. R., Guarino, J. P. and Hamill, W. H., *J. Am. Chem. Soc.* **84**, 4230 (1962).
8. Salmon, G. A., *Disc. Faraday Soc.* **36**, 284 (1963).
9. Smith, D. and Pieroni, J. J., *Can. J. Chem.* **43**, 876 (1965).
10. Portis, A. M., *Phys. Rev.* **91**, 1071 (1953).
11. Castner, T. G., *Phys. Rev.* **115**, 1506 (1959).
12. Pake, G. E. and Purcell, E. M., *Phys. Rev.* **74**, 1184 (1948).
13. Our curve is in substantial agreement with recent data of Lin, J., Tsuji, K. and Williams, F., *J. Am. Chem. Soc.* **90**, 2766 (1968).
14. Kittel, C. and Abrahams, E., *Phys. Rev.* **90**, 238 (1953).
15. Wyard, S. J., *Proc. Phys. Soc.* **86**, 587 (1965).